Low Uncertainty Wave Tank Testing and Validation of numerical methods for Floating Offshore Wind Turbines

Christian W. Schulz[1], Stefan Netzband[1], Philip D. Knipper[1], and Moustafa Abdel-Maksoud[1]

[1]Hamburg University of Technology, Am Schwarzenberg-Campus 4, 21073 Hamburg, Germany

Correspondence: Christian W. Schulz (christian.schulz@tuhh.de)

Abstract. The accurate simulation of loads and motions of Floating Offshore Wind Turbines (FOWT) in operation is key to the commercialisation of this technology. To improve such load predictions, a critical assessment of the capabilities and limitations of simulation methods for FOWT is mandatory. However, uncertainties arise during the whole validation process of a numerical method. These can drastically impair the quality of the validation. In the case of FOWT, the interaction between aerodynamic,

5   hydrodynamic and mooring loads on the one hand and platform motions on the other hand causes a high level of uncertainty in the measurement data acquired in model tests. This also applies to comparing a numerical model to the test data, as these interactions make the distinction between cause and effect challenging. To address these challenges, several improvements to the validation process aiming at the reduction of the uncertainties are proposed and evaluated in this work. The major improvements are the measurement of the rotor thrust force excluding the tower top inertia loads, a significant improvement of

10   the wind field quality in the wave tank and the utilisation of hybrid simulations based on the measured platform motions. These steps are applied to wave tank tests of a FOWT utilising a single point mooring and the subsequent validation of the numerical panel method *pan*MARE. The improvements allowed for a considerable decrease in the random and systematic uncertainty of the model tests and made a valuable contribution to the distinction between cause and effect regarding the deviations between measurements and simulations.

1   Introduction

The ability to perform precise and reliable simulations of the motion behaviour of Floating Offshore Wind Turbines (FOWT) is a key requirement for developing resource- and cost-effective designs. Numerous methods for simulating FOWT dynamics with very different degrees of complexity have been developed. However, a critical assessment of the modelling inaccuracies and expected deviations from simulated to real loads of the various simulation approaches is necessary. A starting point for this

20   validation process is the generation of measurement data in model tests. Here, the interaction between the hydrodynamic loads on the floating platform, the tension of the mooring lines and the aerodynamic loads acting on the rotor is reproduced in the wave tank. The obtained motions and loads can then be compared to simulation results to identify, quantify, and understand the observed deviations between the experiment and the simulation. Due to the high complexity of the FOWT motion dynamics, multiple challenges arise throughout the validation process, which could potentially impair the quality of the assessment of

25   simulation methods.

A major challenge is the generation of reliable and accurate measurement data. Considerable effort has been undertaken by the research community in the last two decades to provide suitable data sets for validation. However, a relatively high level of systematic and random uncertainty was observed in several experimental studies. This is especially an issue when the complete wind turbine is considered, and a wind field is applied in the wave basin. In this case, referred to as 'full physical testing', the generation of the wind field is a driver of the observed uncertainties.

In addition to the difficulties in practical testing, it turned out to be challenging to clearly link deviations between simulations and measurements to a specific modelling insufficiency of the utilised simulation method. Especially in the case of deviations between measurements and simulations that can be caused by multiple reasons, it is challenging to distinguish between the impacts of the different physical systems on certain loads or motions. As a consequence, it is difficult to clearly understand the physical reasons for such deviations and improve the simulation method accordingly. The measurement of interface loads at the tower top and mooring points can help to mitigate this problem. While this proved to be successful for the mooring loads, it remains challenging to validate aerodynamic loads using tower top measurements because inertial loads due to platform motion and tower vibrations superimpose the measurement signal.

The value of the validation results is also impacted by the choice of load cases as well as the comparison metrics between simulations and measurements. As many wave tank experiments do not exclusively serve as validation cases but also as practical tests for FOWT designs, irregular sea states are often utilised to investigate the FOWT under realistic conditions. In consequence, a time-domain comparison between measurements and simulations is often difficult to realise due to the complexity of these load cases. Frequency domain comparisons like amplitude and power spectral density spectra are suitable for comparisons regarding the general motion behaviour of the FOWT in these cases. However, without the consideration of the corresponding phase spectra, the transformation of experimental and numerical results in the frequency domain results in loosing a part of the information on the transient behaviour and interrelations between motions and loads. While statistical analyses are suitable for the characterisation of the overall motion behaviour, the quantification and identification of simulation inaccuracies arising from insufficient modelling can be challenging when such comparison metrics are used only.

This work aims at an improvement of the described validation process for FOWT simulation methods in order to gain better insight into the modelling deficits and the level of uncertainty that can be expected in FOWT simulations. Thus, a number of potential improvements for the quality of this process ranging from the experimental setup to the comparison metrics are proposed and evaluated. These are in particular:

Reduction of systematic and random measurement uncertainty

- The wind field quality is significantly increased in terms of flow non-uniformity and turbulence intensity. This is achieved by the use of an elaborate wind generator design. The new design leads to a larger size of the wind generator. Due to the limited space in the wave tank, the size of the wind field and, consequently, the wind turbine rotor needs to be reduced while the wind speed is increased in order to achieve a Froude-scaled thrust force.
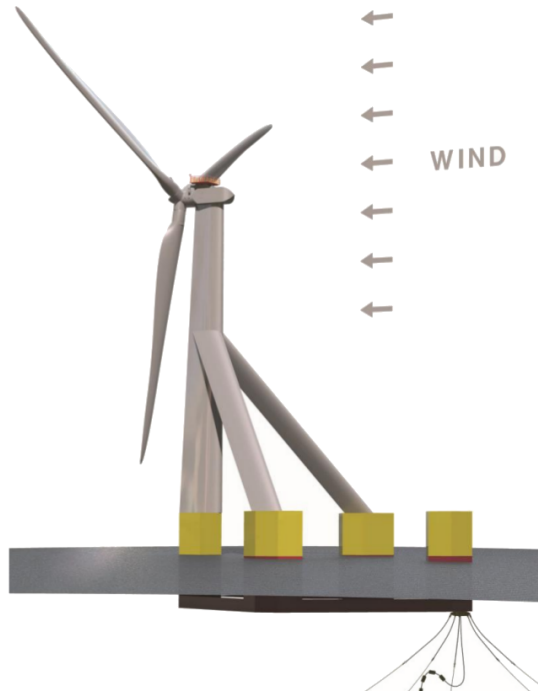
Figure 1. Illustration of the Curse Offshore SelfAligner. Reprinted with permission of CRUSE Offshore GmbH.
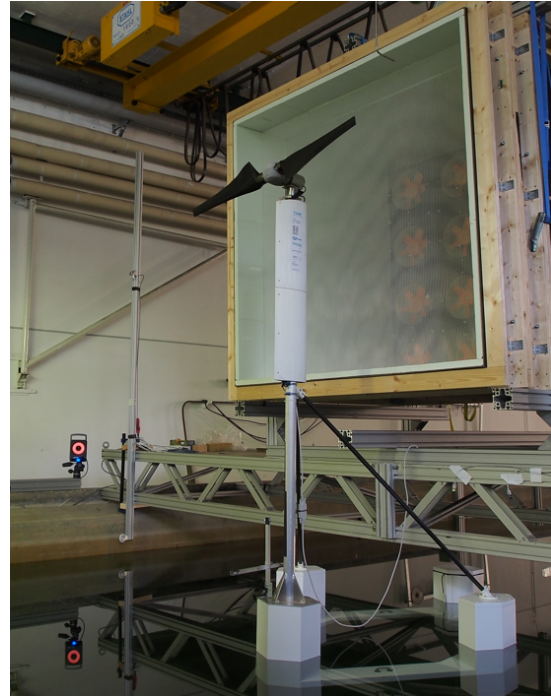
Figure 2. Photograph of the model setup.

- A wireless data acquisition system is utilised to minimise the influence of the cable bundle on the platform motion. The land connection is reduced to a single cable with nearly negligible weight.

- Every measurement case is repeated at least twice in order to continuously monitor the repetition error.

Enabling isolated validation of simulation sub modules

- tower top loads are measured in all three directions, and a procedure to remove the inertial and gravitational loads is applied and validated to determine the aerodynamic thrust force in time domain. Due to the improved quality and a detailed characterisation of the wind field in combination with the measurement of the aerodynamic thrust, a clear identification of the contribution of the aerodynamic loads to the platform motion is enabled.

- The mooring forces in all three directions are measured at the connection of the mooring to the floater.

- Prior to the full validation, a validation of the simulation sub-modules for mooring and aerodynamics is performed. This is realised by the application of the measured platform motion trajectory in the simulation model, which is referred to as 'hybrid simulation'. The results are directly compared to the measurements of the aerodynamic thrust force and the

mooring loads. In this way, the rotor and mooring loads are validated under test conditions but isolated from possible insufficiency in the prediction of the platform motion.

Validation with phase-averaged time-domain measurements

– Simple, periodic load cases are chosen to deliver basic validation data with high accuracy.

75 – Time-domain measurements are obtained using phase-averaging. In this way, a considerably low influence of random uncertainty on the comparison between measurements and simulations can be reached.

In this work, the above-proposed improvements are applied to the validation procedure of the first order panel method *pan*MARE using the Curse Offshore SelfAligner FOWT (see Figure 1), which is passive yaw concept. The wind turbine was downsized by a factor of 3 compared to the scaling of the platform, which yields a smaller wind generator cross-section. A
80 major drawback of this procedure is the violation of the Froude similarity in the time scale of the wind field and the tower top motion. This violation causes a reduced sensitivity of the rotor loads on the tower top motions. Nevertheless, the dynamic effects of platform motions on the rotor loads and vice verca are measured and can be accurately modelled in the numerical method.

85 In the following sections, relevant parts of a number of previous studies are summarised to present the context of this work. Subsequently, the downsizing of the rotor is discussed, and the utilised numerical method, as well as the design of the wind generator, are introduced. Furthermore, the complete wave basin setup is depicted and a series of repetition tests is presented to quantify the expectable random uncertainty. Measurement data is utilised to validate the modules of *pan*MARE and their coupling in hybrid and full simulations. Finally, the findings from the validation and the application of the proposed
90 experimental technique are concluded.

2   Previous works in the field of wave tank testing and validation of numerical methods

A considerable number of experimental investigations on loads and motions of FOWT in model-scale have been performed in the past two decades. Otter et al. (2021), Murphy et al. (2015), Chen et al. (2020) and Gueydon et al. (2020) provide general reviews and an overview of most of these investigations in wave tanks. In these, different ways of considering the aerodynamic
95 loading on the rotor in the context of the scaling issue between Froude similarity on the hydrodynamic side and Reynolds similarity on the aerodynamic side were evaluated. Apart from some early studies utilising a simple drag disk (e.g. Roddier et al. (2010)), the generation of aerodynamic loads in recent works can be divided into three categories: Bottom-fixed thrust generation, hybrid testing and full physical testing. The advantages and disadvantages of the first two approaches are briefly described in the following, while a more detailed view is given on the full physical testing approach as it is most relevant for
100 the present study.

The bottom fixed thrust generation offers a simple way to model at least the mean thrust force and fluctuations of the incoming wind. Here, a predefined thrust force time series is applied to the tower top with the aid of a controlled propeller

(see e.g. Andersen (2016) and Desmond et al. (2019)). The major drawback of this technique is that there is no interaction between the aerodynamic loads and the tower top motion. Consequently, important coupling effects like aerodynamic damping

105 cannot be reproduced in the wave tank tests. The bottom-fixed thrust force generation approach can therefore be considered as a cost-efficient way for the testing of new FOWT designs, but its applicability for the generation of validation data including aerodynamic loading is limited.

A considerable number of hybrid testing devices have been developed and tested in recent years. Otter et al. (2021) provide a detailed review of these devices. To date, two different types of actuators are utilised to apply the rotor loads to the platform.

110 Either propellers or multiple cables connected to winches are mounted on the tower top. Both techniques utilise a real-time numerical simulation of the aerodynamic domain, which is coupled with the measured tower top motions of the platform model. Finally, a feedback loop is created, so that the tower top motions are considered in the aerodynamic simulation while the actual aerodynamic loads are applied to the wave tank model by the actuators. The suitability of the hybrid testing approach for wave tank testing of new FOWT prototypes and validation tests focusing on hydrodynamics was demonstrated in a number of studies

115 (e.g. Azcona et al. (2014), Amaral et al. (2021), Otter et al. (2020), Hall and Goupee (2018), Vittori et al. (2022)). Naturally, a validation of the aerodynamic loads is not possible with this approach. In addition, there is still a lack of investigations on the influence of the time lag between desired and realised tower top loads on the motion behaviour, see Gueydon et al. (2020). Similarly, more investigations of the random uncertainty arising from the actuators are needed to characterise the capabilities and limitations of this approach.

120 **Full physical testing**

To date, full physical testing is an important option to gain validation data for numerical models covering the aerodynamic and hydrodynamic domain. In this approach, a wind generator is placed in the wave tank, and a model rotor is installed on the floating platform. The full physical testing approach is widely used and a number of examples can be found in the above mentioned reviews. In the following, relevant test campaigns and validation studies are briefly described in order to summarise

125 the advantages and issues of this testing methodology.

In most full physical tests, the rotor is not geometrically scaled as special low Reynolds number airfoil shapes are used. In addition, the chord length of the blade sections is increased to achieve a minimum of similarity to the full-scale characteristic of a wind turbine rotor in terms of Reynolds number and blade loading. One of the early studies, the DeepCWind campaign led

130 by the University of Maine in 2011, showed that the utilisation of geometric scaling of the blades lead to a significantly reduced thrust force and an extremely low power output, see Goupee et al. (2014). A redesign of the rotor with airfoils designed for low Reynolds numbers - as used in classical wind tunnel experiments - showed a considerable improvement of the rotor performance and was used in a later test campaign. During the OC5 project (Offshore Code Comparison Collaboration Continued with Correlation) presented by Robertson et al. (2017), measurement data from this campaign was utilised to validate multiple

135 numerical methods. As an uncertainty assessment was not performed during the tests, some consistent deviations between measurements and simulations were not fully understood. A high level of uncertainty in the generated wind field and/or its

measurement, as well as the influence of the instrumentation cable bundle, were proposed as possible explanations for deviations between measurements and simulations. The quality of the wind field was indeed limited in these cases: Maximum spatial deviations from the mean wind speed up to 20 % and turbulence intensities slightly below 10 % were measured across the rotor
140 swept area (Wendt et al., 2019). Wendt et al. (2019) calibrated a simulation model in the FAST simulation framework to match the results of a test campaign on the DeepCWind semi-submersible with the redesigned rotor. The calibration improved the agreement between simulations and measurements. However, issues in the statistically evaluated tower base force remained. A summary of the DeepCWind tests recommended a higher quality of the wind field, as strong non-uniformity was observed, and wireless data acquisition in order to reduce the influence of the cable bundle, see Robertson et al. (2013).

145

Bredmose et al. (2017) performed a full physical test of a novel platform design aiming at the investigation of aerodynamic damping and the influence of the wind turbine controller on the platform motion. A strong effect of aerodynamic damping on the platform pitch and surge response to a focused wave group was shown. In wind-only tests, the effect of negative damping (see Jonkman (2008)) due to the use of an onshore blade pitch controller was demonstrated, while the developed offshore
150 controller did not excite the platform motion. In regular and irregular wave tests, the superior motion damping of the offshore controller could be proved. In a regular wave only condition, exemplary time domain comparisons with a simulation using FAST showed good agreement with the measurements. Flow measurements in the wind field revealed strong non-uniformities and turbulence intensities ranging from below 10 % up to 20 %, while a part of the lower rotor half was not entirely covered by the measurements. As a consequence, high-frequent noise appeared in the thrust force during constant wind tests. In the case
155 of rotor torque, noise was even observed in low-frequency ranges. Finally, the application of the wind field yielded an increase of the scatter in the pitch motion compared to cases without wind.

Yu et al. (2017) presented a test series focusing on the implementation of a controller, including measurements of the tower top loads, using the same model. Steady measurements showed that the results of the aerodynamic simulation model needed to be adjusted by 65 % to match the measured power coefficient. In addition, a large oscillation of the rotor thrust force was
160 monitored in the experiments, which resulted in the occurrence of negative values for the thrust force. Although named as aerodynamic thrust force, it is likely that the gravitational and inertia loads have not been compensated from the signal. Therefore, the tower top force rather than the rotor thrust is probably shown.

Cao et al. (2022) and Wang et al. (2024) also report the usage of an inertia removal procedure applied to tower top force
165 measurements. However, no validation or verification of the procedures and no distinct comparison with aerodynamic simulations is given in these works.

Very recently, 17 participants of the OC6 project (Offshore Code Comparison, Collaboration, Continued, with Correlation and unCertainty)[1], used model tests of the Tetraspar FOWT as a basis for a broad validation study with 15 different simulation
170 methods (see Bergua et al. (2023)). The validation campaign showed a promising overall agreement between the measurements

---

[1]https://iea-wind.org/task30/, last accessed on 2nd April 2024

and the different simulation models. However, it was found that the cable bundle had a significant influence on the motion of the platform, and the simulations had to be corrected for this influence. Although tower top loads have been recorded, an explicit validation of aerodynamic loads under wave excitation has not been performed.

In summary, the full physical testing approach was applied successfully to various different FOWT concepts and provided insight into their motion dynamics. As an example, the presence of aerodynamic damping could be proved in several studies. However, general issues regarding the quality of the measurements and the wind fields were reported. For example, Robertson (2017) claimed that more repeat tests in wave tank testing of FOWTs are necessary to investigate the random uncertainty as a consequence of the DeepCWind measurement campaign. Unfortunately, publications containing consequent repetitions of the tests are still rare. Similarly, Gueydon et al. (2020) recommended accumulating more evidence on the validity of the applied testing methodology in the context of measurement uncertainties. Many works report issues on the quality of the wind field, although considerable effort was undertaken to manufacture elaborate wind generators in a large scale. In addition, investigations of the tower top loads have been performed in few studies, so the consequences of the quality issues in the wind fields are difficult to quantify. It is likely that a considerable portion of the random uncertainty observed in the above studies arises from undesired flow non-uniformity and high turbulence intensity in the wind field. A compensation of inertia loads to directly evaluate the rotor thrust or torque seems to be rare, if even present.

In most cases, comparisons of numerical and experimental results are performed on the basis of statistically evaluated amplitude spectra, which may not tap the full potential of the information gained from the experiments. As statistical values are comparably insensitive to noise, a possible reason for the choice of these evaluation methods could be that the random uncertainty in the measurements makes accurate time domain investigations challenging. In addition, the performed validation studies focus on simulations utilising frequency domain methods in terms of hydrodynamics. Comparing those results to measurements in frequency domain may yield better performance than can be expected in time domain because these methods use similar frequency domain results from higher fidelity methods as input.

3 Scaling

Previous studies showed that the design and manufacturing of large-size wind generators with high flow quality is an extremely challenging task. Therefore, a reduction of the rotor size - resulting in a reduction of the wind generator size - is applied in order to allow for a more elaborate wind generator design. In the following section, the consequences of this approach on the similarity to the full-scale FOWT in terms of Froude similarity are discussed.

To maintain the similarity between the motion behaviour of the scale model and the full-scale FOWT, a similarity of gravitational and inertial loads (Froude similarity) is primarily required. This is due to the fact that ocean waves and the rigid body motion of a floating body are mainly driven by gravitational and inertia effects. However, usually, it is not possible to concurrently maintain Reynolds similarity due to the absence of a model fluid with a suitable kinematic viscosity, see Hughes (1993). For most floating bodies, viscous forces like drag do not have a driving influence on the floating motion and can, therefore, be

disregarded, approving a certain error or artificially modelled in numerical models to match experimental data. In contrast to
this, viscous effects are most relevant for wind turbine aerodynamics. The violation of the Reynolds similarity leads to strong
deviations in the aerodynamic loads when geometrical scaling is used. This is due to the difference in the Reynolds numbers at
the blade sections compared to a full-scale turbine, which is extreme in this case. Therefore, downscaled rotor blades usually
need to be redesigned for the low Reynolds number regime in model-scale as already mentioned in section 2. In this way, a
thrust characteristic similar to that of a real wind turbine can be achieved, which fulfils the Froude similarity of the rotor thrust
force. However, in practice, the thrust characteristics of modern wind turbines are quite similar, so the redesigned turbine often
serves as a general representative for a certain power rating rather than reflecting an individual turbine. From this, it becomes
clear that the rotor is not necessarily a model of the full-scale version; however, it can be considered as an external substitute
system that provides suitable aerodynamic loads in terms of Froude similarity.

In the present case, the diameter of the model rotor as a substitute system for thrust and torque generation is not scaled with
the same factor that is used for the platform. A photograph of the downscaled model is shown in Figure 2. While the scaling
factor for the platform and the hydrodynamic environment is $\lambda_{hydro} = 45$, the scaling factor for the wind turbine rotor was
chosen to be $\lambda_{aero} = 150$, as illustrated in Figure 3. In order to maintain the similarity of mean thrust assuming a constant
thrust coefficient and tip speed ratio, the wind speed needs to be increased by the factor $\lambda_{aero}/\lambda_{hydro}$.

As a consequence of the different scaling ratios of the rotor and platform, the kinematic similarity between the tower top
motion velocity due to pitch motion and the wind speed is violated. This leads to a reduction of the sensitivity of the rotor
thrust to the platform motion. For a harmonic surge motion, the thrust force amplitude is reduced by the factor $\lambda_{hydro}/\lambda_{aero}$
in comparison to the full-scale scenario. A detailed derivation is given in appendix A. In the present case, the amplitude is
approximately reduced by a factor of 3. A comparison of the rotor thrust of the full-scale FOWT and the proposed scale model
undergoing a sinusoidal surge motion is shown in Figure 4. As a result, the effect of aerodynamic and hydrodynamic interaction
phenomena like aerodynamic damping is reduced; however, it is well-defined and can be observed in the platform motion and
the tower top load measurements. Therefore, even though the Froude similarity of tower top motion velocity and wind speed
is violated, the utility system is well suited for the validation of numerical methods.

4 Test setup and measurement system

The model tests were performed in the 5 m wide and 80 m long towing tank of the Hamburg University of Technology. A
platform was mounted over the water to accommodate the wind generator. The scale model of the FOWT and the wind
generator were placed in the first third of the wave tank and aligned with its centre line.

In this section, the wind generation system, the physical model, the used sensors and data acquisition system is described.
Particular emphasis is put on the investigation of the wind generator performance and the acquisition of the inertia force
compensated rotor thrust force.
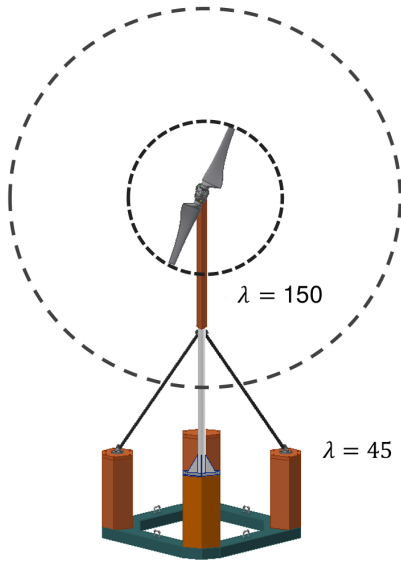
Figure 3. Sketch of the applied scaling ratios.
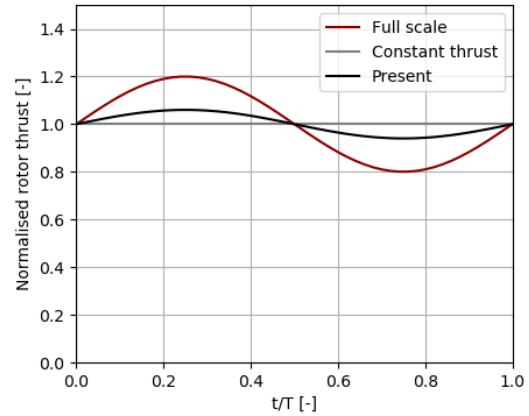
Figure 4. Illustration of the expected deviations in the normalised aerodynamic rotor thrust from full-scale to the present approach during an exemplary surge oscillation.
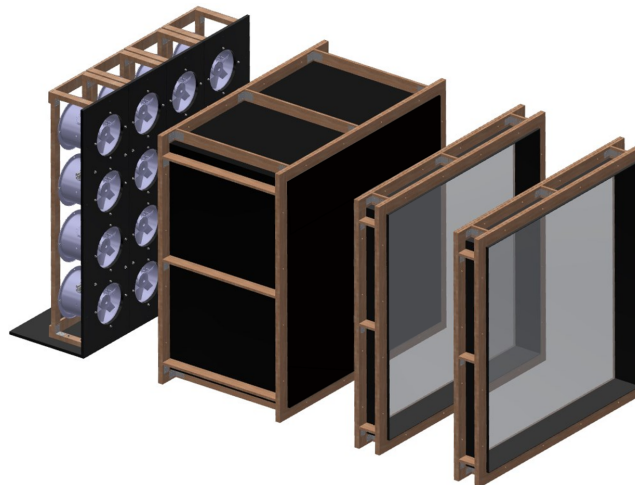
Figure 5. Illustration of the wind generator assembly.

4.1 Wind generator

A modular, lightweight and easy-to-install wind generator has been designed and manufactured (see sketch in Figure 5). With an outlet cross section of 1.6 m by 1.6 m, the rotor is more than fully covered. The wind generator consists of an array of 16 fans, a settling zone with a length of 1 m and two mesh screens at a distance of 0.2 m and 0.4 m to the outlet. The mesh screens consist of a rectangular grid of polyamide threads with a diameter of 0.39 mm and have an overall porosity of 62 %.

240 The modules (four fan rows, one settling zone, two screens) are mounted using a wooden frame and can be combined in any order and with additional elements. However, no modular division of the wind generator cross-section was undertaken in order to avoid the introduction of flow non-uniformity between such modules. All modules can be easily handled by two persons so that the wind generator can be assembled on the platform over the wave basin without the need for extra equipment.

The 16 fans are powered by a frequency inverter, which can be controlled in closed-loop control with a velocity measurement 245 using a Prandtl probe. However, it turned out that the slip of the asynchronous motors stays constant after a short initial warm-up so that the control of the supply frequency via the inverter is sufficient to maintain a constant wind speed. The Prandtl probe was therefore utilised to monitor the actual wind speed. Air pressure, temperature, and humidity were recorded prior to every test to monitor the air density and its influence on the wind turbine loads as well as on velocity measurements.

The generated wind field was investigated on a plane with a distance of 1.2 m to the outlet using a Prandtl probe, which was 250 mounted on a frame that allowed for an exact positioning of the 102 measurement points. Every point measurement was performed for 10 s, and the mean wind speed, as well as the turbulence intensity, have been calculated. The signal was sampled with a frequency of 1.2 kHz and low pass filtered by 350 Hz in order to exclude measurement noise but still consider fluctuations induced by the fan blades. In Figure 6, average wind speed and turbulence intensity are illustrated from an interpolation between the measurement points. For the average wind speed, a maximum deviation of approximately 2 % between a single 255 measurement point and the mean wind speed inside the denoted rotor swept area was observed. The turbulence intensity in this region was found to be below 5 %. Even though the flow quality slightly decreases towards the boundaries of the wind field, a high homogeneity can be maintained even if the rotor undergoes small motions.

Additional investigations showed that the sensitivity of the average wind speed and turbulence intensity to a variation of the 260 distance to the wind generator outlet (0.8 m up to 1.6 m) is very limited. Slight changes in the wind speed, i.e. fan frequency, also did not cause significant deviations in the wind field quality. When removing one mesh screen, both maximum flow non-uniformity and turbulence intensity increased significantly. Initially, baffle plates were installed inside the settling zone in order to reduce potential rotation in the flow field. As a result, it was found that the maximum deviation from the mean wind speed increased drastically. This can be explained by inaccuracies in the baffle plate's geometry and positioning. Therefore, the baffle 265 plates have been removed.

Apart from the size, the main differences in the wind generator design and configuration in comparison to similar devices can be summarised as follows:

– The wind generator outlet cross section is nearly twice as wide and high as the rotor diameter.

270 – No subdivision of the wind generator's cross-section is created either by modularisation, baffle plates or support structures.

– A comparably large settling zone is present.

(a)   (b)
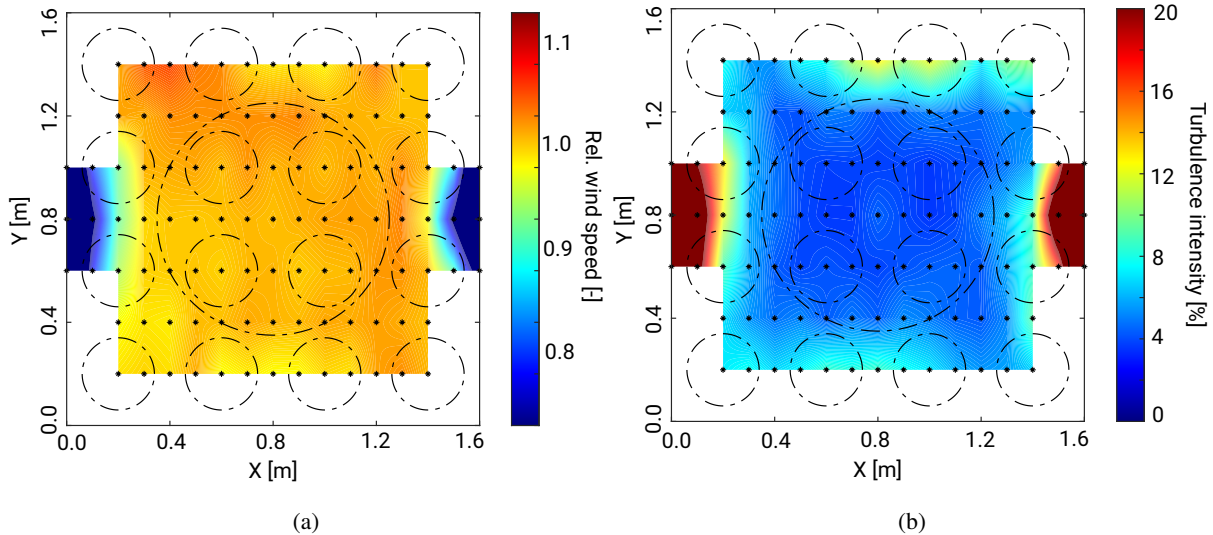
Figure 6. Velocity field measurements interpolated from from 102 measurement positions. (a) Normalised average wind velocity; (b) Turbulence intensity. Small dashed circles indicate the positions of the fans, while the large circles indicate the rotor-swept area. Measurement points are marked by black dots.

- Two fine, homogeneous mesh screens without any support structures inside the wind generator cross-section were utilised.

275 - An average distance of slightly more than one rotor diameter between the rotor and the wind generator outlet was maintained during the model test.

4.2 Model details

A model of the CRUSE Offshore SelfAligner platform (see Figure 2) utilising a single point mooring (SPM) and a downwind rotor was developed and manufactured. Due to the absence of a yaw mechanism and the ability to turn around the mooring 280 point, the SelfAligner can be considered a passively yawing FOWT concept. The tower is equipped with an airfoil to support the passive yaw mechanism. A numerical study on the passive yaw capabilities has been presented by the authors in 2020; however, the yaw mechanism is not the focus of this work.

The lower part of the platform (i.e. bottom plate and columns) consists of CNC-milled polyurethane foam with different 285 densities for the bottom plate and columns. Therefore, the geometry and mass distribution of the underwater parts are known exactly, and no deviation due to the soaking of water is expected over time. Inside the hollow columns, fine ballast weights and measurement equipment are stored. The tower consists of an aluminium pipe with carbon fibre bracings connected to the middle columns, which ensure a high tower eigenfrequency far from the wave frequencies. The upper part of the tower subjected

to the wind is equipped with an airfoil-shaped cover to maintain a parallel alignment of the platform with the wind.

290

The two-bladed downwind model wind turbine has been used in wind tunnel investigations focusing on the yaw moment prior to the wave tank tests. A detailed description of the rotor with a diameter of 0.93 m can therefore be found in Schulz et al. (2022). The same rotor has also been used for an investigation of the unsteady aerodynamic phenomena during a surge motion in the wind tunnel (after the present test campaign), see Schulz et al. (2024). The blades were redesigned for a low Reynolds

295 number regime. However, due to the increased chord length, a comparably high Reynolds number $75x10^3$ at the blades and a power coefficient of approximately 0.35 could be achieved. In order to prevent undesired blade bending, the blades were manufactured using carbon fibre prepreg around a CNC-milled hard resistance foam core with carbon fibre shear webs. A 3D scan of both blades showed negligible manufacturing deviations. A Kollmorgen TBM brushless motor powered by a Kollmorgen AKD controller maintained a constant rotational speed during the tests.

300

The mooring system had to be redesigned with very short mooring lines due to the limitation of the towing tank width. Therefore, a similarity to the full-scale system could only be maintained in the static downpull of the mooring system, while the stiffness in the vertical and horizontal directions is different. Commercially available chains (DIN 5685 1/C 30) with a wire diameter of 3 mm kept the scale model in place. However, as no exemplary site was chosen, no specific characteristics of the

305 mooring system had to be fulfilled in the model tests.

The determination of the mass and inertia properties of the wave tank model is described in appendix B.

4.3 Sensing system and data acquisition

Motions of the platform in all six degrees of freedom, mooring forces in all three directions, tower top forces and moments in

310 all three directions, rotor speed, wave elevation and wind speed have been continuously monitored during all tests. As reported Robertson et al. (2017) and others (e.g. Ahn and Shin (2019)), the typical cable bundle supplying the measurement equipment and the wind turbine may introduce non-negligible systematic and random uncertainties to the platform motion. Therefore, a wireless data acquisition system was utilised. A detailed description of the sensors and data acquisition system is given in appendix C.

315

In order to obtain the aerodynamic loads from the tower top measurements, compensation for the inertial and gravitational loads acting on the tower top sensor is necessary. As rotor thrust is of primary interest, the rotor nacelle assembly (RNA) was reduced to a point mass located at the RNA centre of gravity (COG). Then, the instantaneous position of the RNA COG was computed from the measured rigid body position of the model. A simple finite difference method was applied twice, yielding

320 the acceleration of the RNA COG. However, a low pass filter with an edge frequency of 5 Hz was applied to the position signal and the calculated inertia force to reduce noise. This filter frequency is approximately five times higher than the maximum motion frequency and is therefore considered to introduce no systematic error to the rotor thrust. In addition, gravitational

Table 1. Load cases in regular waves.

Load case	model-scale			full-scale		
	Wave period	Wave height	Wind speed	Wave period	Wave height	Wind speed
LCA 1	1.19 s	0.11 m	0 m/s	8 s	5 m	0 m/s
LCA 2	1.64 s	0.18 m	0 m/s	11 s	8.1 m	0 m/s
LCA 3	2.09 s	0.18 m	0 m/s	14 s	8.1 m	0 m/s
LCB 1	1.04 s	0.07 m	5 m/s	7 s	3.1 m	10 m/s
LCB 2	1.19 s	0.11 m	5 m/s	8 s	5 m	10 m/s
LCB 3	1.49 s	0.07 m	5 m/s	10 s	3.1 m	10 m/s
LCB 4	1.64 s	0.18 m	5 m/s	11 s	8.1 m	10 m/s
LCB 5	1.79 s	0.11 m	5 m/s	12 s	5 m	10 m/s
LCB 6	2.09 s	0.18 m	5 m/s	14 s	8.1 m	10 m/s
LCB 7	2.30 s	0.20 m	5 m/s	15.4 s	9 m	10 m/s

loads arising from the inclination of the tower top have also been compensated from the tower top measurements. A hint on the accuracy of the applied compensations can be found in Figure 10, where phase-averaged measurement results (red) of three

325 test cases with waves and without wind are presented. It is shown that the rotor thrust could be compensated to zero with a residual of below 0.2 N for the two cases with higher waves and a slightly higher residual for the case with lower wave height. This corresponds to an expected deviation of approximately 3 % of the mean thrust force during operation.

4.4   Load cases

330 In order to keep the comparison of measurements and simulations as clear and simple as possible, only regular wave cases are presented in this study. A number of wave periods and heights distributed broadly over the expected environmental conditions have been chosen and listed in Table1. Emphasis was put on the cases, including slightly below-rated wind, where a high thrust force occurs and the blade pitch controller is not active.

5 Numerical model

335 The model tests were primarily carried out to provide reliable validation data for the first-order panel method *pan*MARE, which was developed at the Hamburg University of Technology. An extension of the method, which has originally been utilised to calculate the motion behaviour of ship hulls and the loads on ship propellers, to a complete framework for FOWT simulations has been presented by Netzband et al. (2018). A unique feature of this method is the utilisation of the same potential flow solver for both, aerodynamic and hydrodynamic, flow fields. In the following, a very brief description of the modelling features is

340 given, while details can be found in the above-mentioned work by Netzband et al..

*pan*MARE solves hydrodynamic, aerodynamic and mooring-induced loads as well as the motion of the FOWT in time domain. This is a major difference to frequency domain potential flow methods that are often utilised to create inputs for conventional coupled FOWT simulation methods (e.g. for OpenFast with HydroDyn). In this way, the capability of the method to accu-

345 rately predict fluid loads during aperiodic or large motions and excitations is improved in comparison to conventional FOWT simulation methods. For example, the instantaneous wetted surface of the platform is considered in every time instant, which is not the case in most other FOWT simulation methods. However, this investigation does not consider a deformation of the water surface due to an interaction with the platform. Computing aerodynamic and hydrodynamic flow fields in the same solver allows for a strong coupling of the methods: The 4th-order Runge-Kutta time marching scheme is applied to all sub-models,

350 so that all intermediate steps of the Runge-Kutta scheme are performed simultaneously without a need for additional coupling steps (except for the mooring system).

Pressure forces on the platform hull and the blade surface are determined from the modelled flow fields. However, the underlying potential theory does not account for viscous forces. Therefore, in the hydrodynamic domain, the drag of the platform

355 parts is modelled with drag elements based on empirical coefficients. As the drag coefficients in the model test are significantly higher compared to the full-scale situation, the coefficients for the simulation model are adjusted to match the decay tests described in the next section. In the aerodynamic domain, the drag force acting on a discretised blade section is calculated on the basis of airfoil drag coefficients, local angle of attack (AoA) and local flow velocity. As described in the previous sections, viscous contributions to the blade loads are dramatically increased in comparison to a full-scale wind turbine. As a correction

360 of the lift force on the basis of empirical coefficients will only correct the blade loads but not the vortex strength shed into the wake, this method is not applicable. The effect of viscosity on the lift curve over the AoA can be simplified to a constant offset of the AoA in the case of the utilised SD7062 airfoil when considering the low AoA region. As the AoA over the blade span is consistently overpredicted in this region, a constant offset of the blade pitch angle of 1° is applied. This offset directly translates to the AoA and can, therefore, be considered as viscous correction for the nominal operational state of the model

365 wind turbine.

6 Repeat tests

All tests from Table 1 have been repeated at least once in order to get a hint on the expectable repetition error. For certain load cases, a second repetition was performed. However, these showed very similar deviations and are not shown here for the sake of a clear illustration. The load cases LCB 2, 4 and 6, including short, intermediate and long wave periods, are analysed in detail using phase-averaged data. As the repetition error strongly depends on the wave excitation, the analysis of the repetition error is also performed using these three exemplary load cases. In Figure 7, wave elevations, selected platform motions and selected force measurements recorded for each load case and two test runs each are plotted. The red and orange lines illustrate the phase-averaged quantities computed from a minimum of five motion cycles for both test runs. Multiple periods of the time domain signals are indicated as black and grey dots. All loads and motions are shown as absolute values in model-scale in order to allow for the evaluation of relations between mooring, tower top loads and surge motion directly. This illustration is also used in the following plots containing phase-averaged data.

The phase-averaged wave elevation shows nearly no deviation between the two test runs. However, in 7a, a slightly increased scattering of the time signal is noticeable. Concurrently, the wave shape does not follow the intended sine function, which indicates that the wave maker is driven near its limitations. Interestingly, the same wave input produced a different wave shape during the wave-only load cases, which are shown in Figure 10a. However, the repetition of this case showed the exact same wave shape. Therefore, it is likely that the internal configuration of the wave maker was slightly changed between the two. This effect seems to be limited to this load case, as the other wave configurations could be reproduced in a satisfactory manner. In 7a, a high scattering of the surge motion in comparison to its amplitude can be noticed, which is due to a slow drift motion arising from the start of the wave maker. However, the surge motions are very small in this case. The remaining platform motions could be reproduced with a very low repetition error and an increased scattering when considering the lowest wave period. In the illustrations of the aerodynamic rotor thrust, a significantly stronger scattering can be seen. This arises from the superposition of aerodynamic, inertia and gravitational forces in the measurement of the tower top force in wind direction. The random uncertainty occurring in the measurement of the significantly higher inertia loads cannot be compensated during the calculation of the rotor thrust force and, therefore, adds considerable scattering to it. In the wave-only cases in Figure 10, the residual rotor thrust force is shown. However, the observed scattering in the repetition tests is slightly higher, which leads to the conclusion that the aerodynamic thrust also adds a part to the random uncertainty. At the lowest wave period, the compensation of inertial and gravitational forces seems to be unable to properly reproduce the variation of the thrust force due to the tower top motion, while a satisfactory repetition error could be reached in the other load cases. Therefore, the calculated rotor thrust has to be considered carefully at low platform excitations. The vertical mooring force could also be reproduced with a low repetition error. In summary, the absolute phase-averaged repetition error and scattering do not vary strongly from case to case, which yields stronger relative deviations for cases with less prominent platform motions.
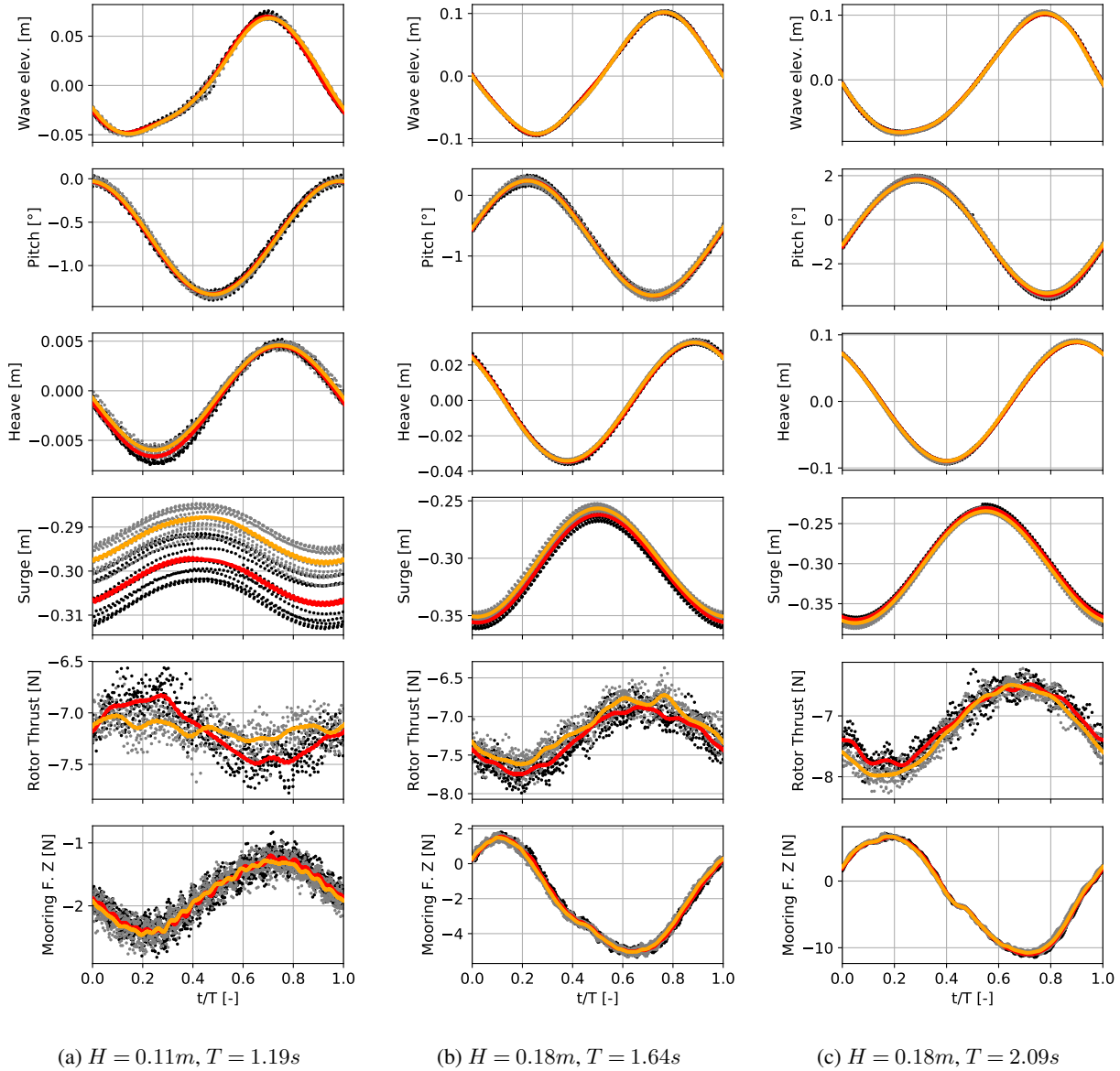
Figure 7. Waves and wind: Repetition tests at three different wave conditions (wave height H and period T). Experiment 1st run: ⋯⋯⋯ and ▬▬▬ (averaged); Experiment 2nd run: ⋯⋯⋯ and ▬▬▬ (averaged).

7 Results

400 The comparison and analysis of the experimental and numerical results is divided into four sections. First, the damping behaviour and eigenfrequencies of the platform are evaluated in decay tests. Second, phase-averaged results of hybrid simulations and the corresponding measurements are presented to separately examine the contribution of inaccuracies arising from the

mooring and aerodynamic simulation modules in three cases. Third, the differences between full simulations and experiments in the same three cases are examined with and without wind during one phase-averaged motion cycle. Finally, the normalised
405 motion amplitudes of all cases with wind are examined in order to examine the influence of the motion frequency on the inaccuracies of the simulation model.

7.1 Decay tests

410 Decay tests in heave, surge and pitch were performed. In the case of heave decay, the mooring system was not connected to the floater in order to identify the heave damping separately from the pitch motion, which would have been introduced by the mooring system. From the decay tests in heave and pitch in Figure 8a and 8b, it can be concluded that eigenfrequencies, as well as motion damping in both directions, can be predicted accurately in the simulations. In the surge direction, a slightly larger difference in the eigenfrequency in the simulation and experiment was observed, while the damping could be precisely met. A
415 slight mismatch of the eigenfrequency indicates that the mooring stiffness in the surge direction is slightly overpredicted. From a comparison of the mooring loads in surge and heave direction, it is obvious that a strong pitch-surge coupling is present. This coupling cannot be exactly reproduced in the simulation. Although not directly visible in these results, a pitch-heave coupling is evident from the excentric application point of the SPM. Therefore, a coupling of heave, pitch and surge motion is likely to strongly influence the motion behaviour of the considered FOWT. During the surge decay, the mooring force in the heave
420 direction is not met properly, which is due to the extremely low motion amplitude.

7.2 Hybrid simulations

In Figure 9, measurement results and simulated forces from hybrid simulations are shown. In these cases, the simulation model
425 synchronously undergoes the exact same rigid body motions as the experiment. In the upper two rows of the picture, the compensated rotor thrust force and the originally measured tower top force in the surge direction are shown. A consistent underprediction of the average rotor thrust of approximately 7 % is apparent for all three wave periods, which is in line with observations under steady conditions. This is also the case in the tower top force. However, it is barely visible due to the oscillation amplitude, which is nearly one order of magnitude higher compared to the rotor thrust. From the ratio of the tower
430 top force and the rotor thrust amplitudes, it becomes obvious that comparably small uncertainties in the tower top force may fundamentally impair the quality of the rotor thrust measurement. However, the amplitudes of rotor thrust force and tower top force seem to be captured well in all three cases. The meaningfulness of the good agreement of the rotor thrust force in 9a may be doubted because the repetition of the measurement showed different behaviour in Figure 7a.

Stronger deviations between measurements and simulations were observed in the mooring loads. An atypical, high-frequent
435 behaviour can be seen in the measured forces, especially in the horizontal direction. The simulations show a similar dynamic

(a)   (b)   (c)
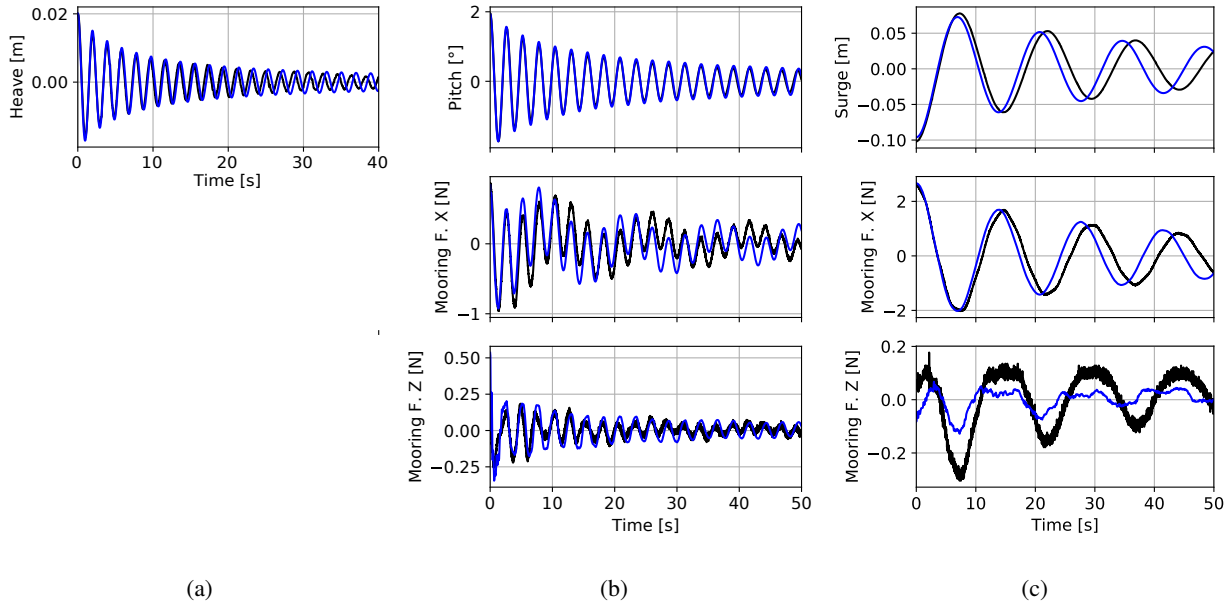
Figure 8. heave (a), surge (b) and pitch (c) decay tests. Experiment: ——— ; Simulation: ——— .

behaviour. However, strong differences in the minimum and maximum force in the surge direction are present. In addition, the previously mentioned slow surge motion at the lowest wave period introduced a large scatter in the phase-averaged diagram. In the heave direction, an acceptable match of the minimum and maximum force could be achieved.

In summary, an atypical behaviour of the mooring system and a poor match of simulations and measurements in surge direction

440   can be stated for the mooring loads. It is likely that the extremely short mooring lines due to the limited space in the towing tank caused this behaviour, which is obviously beyond the limitations of the lumped mass mooring method.

7.3   Full simulations

Measured and simulated motions and loads of LCA 1, 2 and 3 in waves without wind (corresponding to LCB 2, 4 and 6 with

445   wind) are shown in Figure 10. The obvious distortion of the wave shape in LCA 1 has already been discussed in the repeat tests section. The simulated airy waves were abstracted from the measured wave elevation and applied at the exact position of the wave sensor in the simulation. The accuracy of this method has not been investigated in detail, which implies that only a rough comparison of the phases between measured and simulated motions can be performed. Furthermore, the comparison of the wave elevations reveals that the waves applied in the numerical method do not exactly match the measured surface elevation, which

450   is a potential factor in increasing the accuracy of the simulations. A satisfactory match between simulations and measurements of the motions in shape, amplitude and phase is achieved, whereas the pitch amplitude tends to be overestimated, and the heave amplitude tends to be underestimated at higher motion periods. This indicates that the heave-pitch (or heave-pitch-surge)

(a) $H = 0.11m, T = 1.19s$ (b) $H = 0.18m, T = 1.64s$ (c) $H = 0.18m, T = 2.09s$
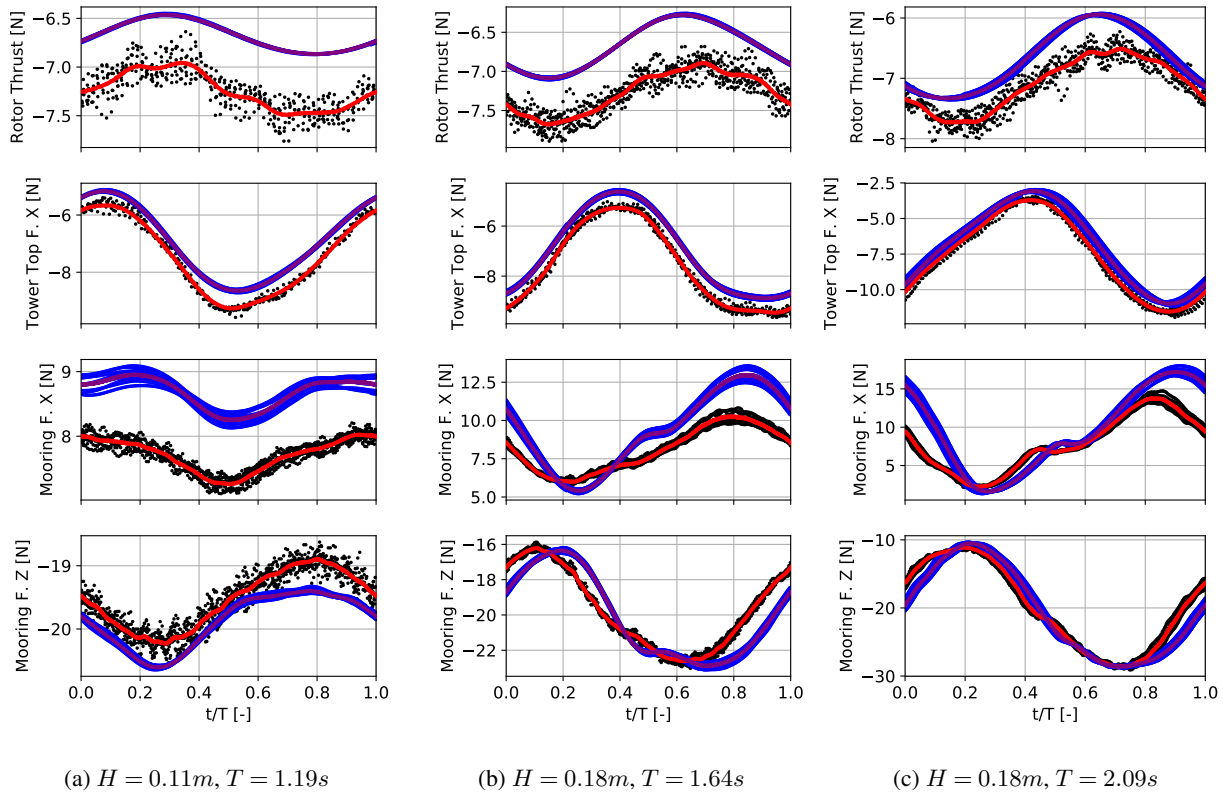
Figure 9. Waves and wind: Hybrid simulations and experimental results at three different wave conditions. Experiment: ·········· and ——— (averaged); Simulation: ·········· and ——— (averaged).

coupling is not exactly captured in the simulations. As the single point mooring is a major contributor to this coupling, it is likely that the mismatch of the mooring loads, revealed by the hybrid simulations, is responsible for this issue. With a rising

455   wave period, the simulated mean surge drift rises stronger than observed in the experiments. This offset in the surge direction can be explained by the mean mooring force in the surge direction, which makes clear that the numerical model is unable to accurately predict the mean wave drift forces. A possible source of this modelling inaccuracy is the application of first-order waves and the neglect of the deformation of the water surface induced by the platform, which may lead to a wrong contribution of the pressure forces to the surge force. While the mooring forces in the vertical direction are met with an acceptable error for

460   LCA 2 and 3, a considerable relative deviation between the maximum values is present in LCA 1. In addition to the general modelling issues regarding the mooring system, the difference in the mean surge position may also play a role here. Apart from the surge mean value, differences in a similar magnitude between experiment and simulation can be found in the mooring loads when considering the full and the hybrid simulations. Therefore, it is evident that a considerable part of the modelling inaccuracies observed may be ascribed to the scaling issues of the mooring rather than to issues in the hydrodynamic simulation
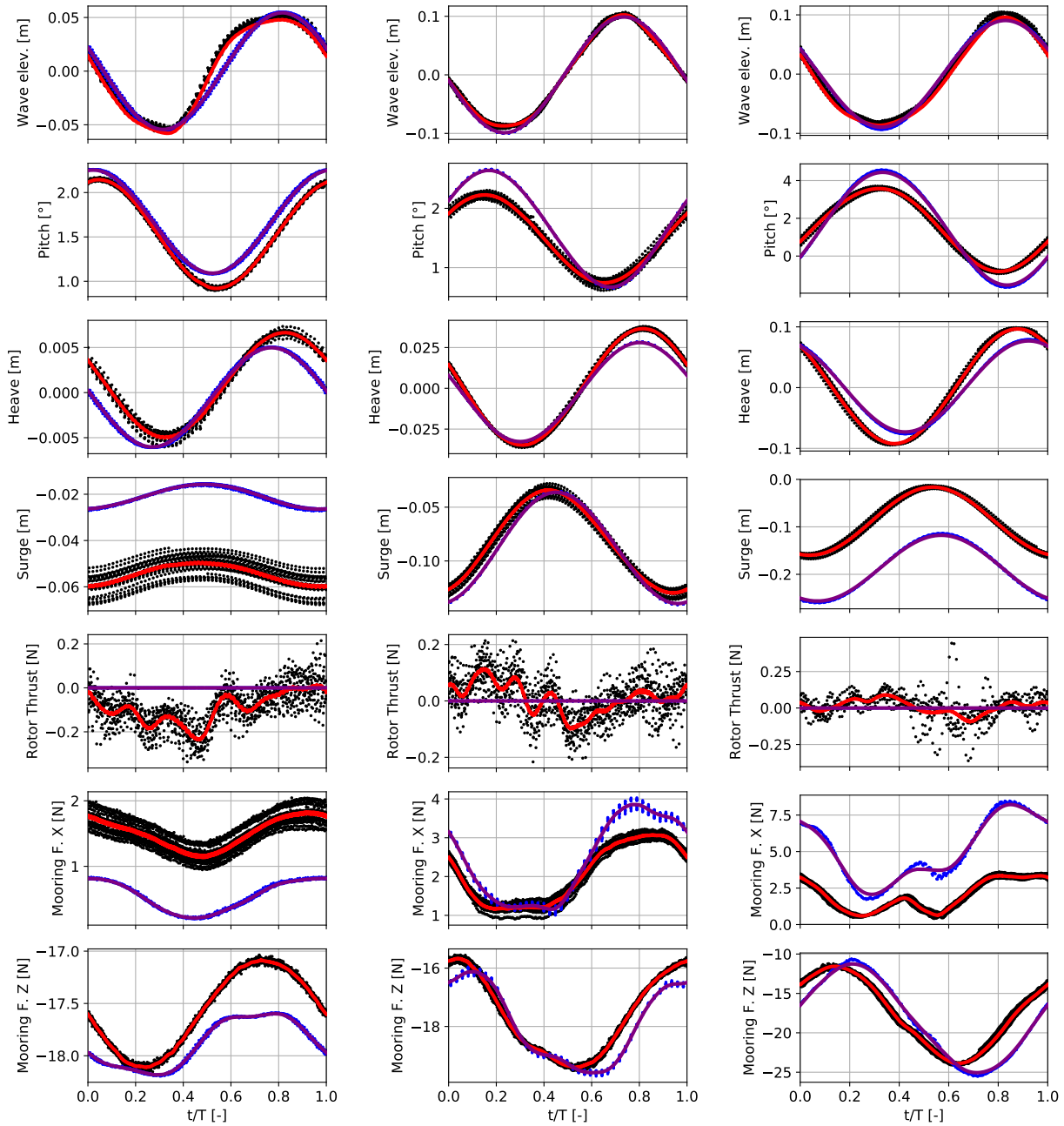
Figure 10. Waves only: Full simulations and experimental results at three different wave conditions. Experiment: ·········· and ———— (averaged); Simulation: ·········· and ———— (averaged).

465   or coupling.

The same wave conditions but including a wind field with a velocity slightly below the rated wind speed of the turbine were applied in LCB 2, 4 and 6, which are shown in Figure 11. When considering the time domain signals indicated with black dots, the applied wind field caused an increase of absolute scattering in the mooring forces compared to the wave-only
470   cases. Nevertheless, no significant changes in the scattering can be seen in the motions. Overall, an agreement of simulated and measured platform motions comparable to the wave-only cases could be achieved, as the pitch and heave amplitudes are again slightly over- i.e. underestimated. The mean value and fluctuation of the rotor thrust force due to the tower top motion are clearly visible in the measurements and cause an offset of the mean surge position and pitch angle in all cases. In addition, the minimum aerodynamic thrust occurs during the forward surge and pitch motion, which clearly indicates the presence of
475   aerodynamic damping. However, when comparing the measured and simulated thrust force amplitude, an overestimation, rising with the wave period, is apparent. As this clear overestimation is not present in the hybrid simulations, it is most likely that this mismatch is caused by the higher simulated amplitude of the tower top motion in the surge direction due to the platform pitch and surge motions.

Compared to the wave-only cases, an increase in the pitch motion amplitude due to the presence of wind can be noticed. This
480   contradicts the above-mentioned observations and experiences from other experiments, where the aerodynamic damping reduced the platform pitch amplitude. The influence of the mean thrust force on the mooring system may provide an explanation for this. While the platform undergoes similar surge motions in with and without-wind cases, the mooring force amplitude in the surge direction is more than doubled. It can, therefore, be concluded that the mooring stiffness has increased drastically due to the mean surge deflection. As a consequence, the effect of heave-pitch-surge coupling induced by the single point mooring is
485   increased, which finally overcompensates the aerodynamic damping and leads to a stronger pitch motion. As discussed in the previous sections, the mooring system could not be scaled properly, such that the stiffness in the surge direction is especially much stronger than in reality. In addition, the influence of aerodynamic damping is reduced due to the downscaling of the rotor. It is, therefore, unlikely that the aerodynamic damping is overcompensated in such a way in full-scale. However, the increased influence of heave-pitch-surge coupling on the platform pitch due to the presence of wind should also be considered
490   in full-scale. From the comparison, it could be demonstrated that the simulation is generally able to capture the effect of a mean surge deflection on the heave-pitch-surge coupling but suffers from deviations in the absolute mooring forces.

7.4   Motion amplitudes

In Figure 12, the motion amplitudes obtained from load cases LCB 1-7 are shown normalised by the wave elevation. As heave
495   and pitch eigenfrequencies are located towards the higher wave periods, an increase in the motion response is visible in heave and pitch with a rising wave period. The identified issues in reproducing the mooring loads leading to a deviated contribution of the heave-pitch-surge coupling to the platform motion can also be seen in this illustration. Nevertheless, an overall good

(a) $H = 0.11m, T = 1.19s$ (b) $H = 0.18m, T = 1.64s$ (c) $H = 0.18m, T = 2.09s$
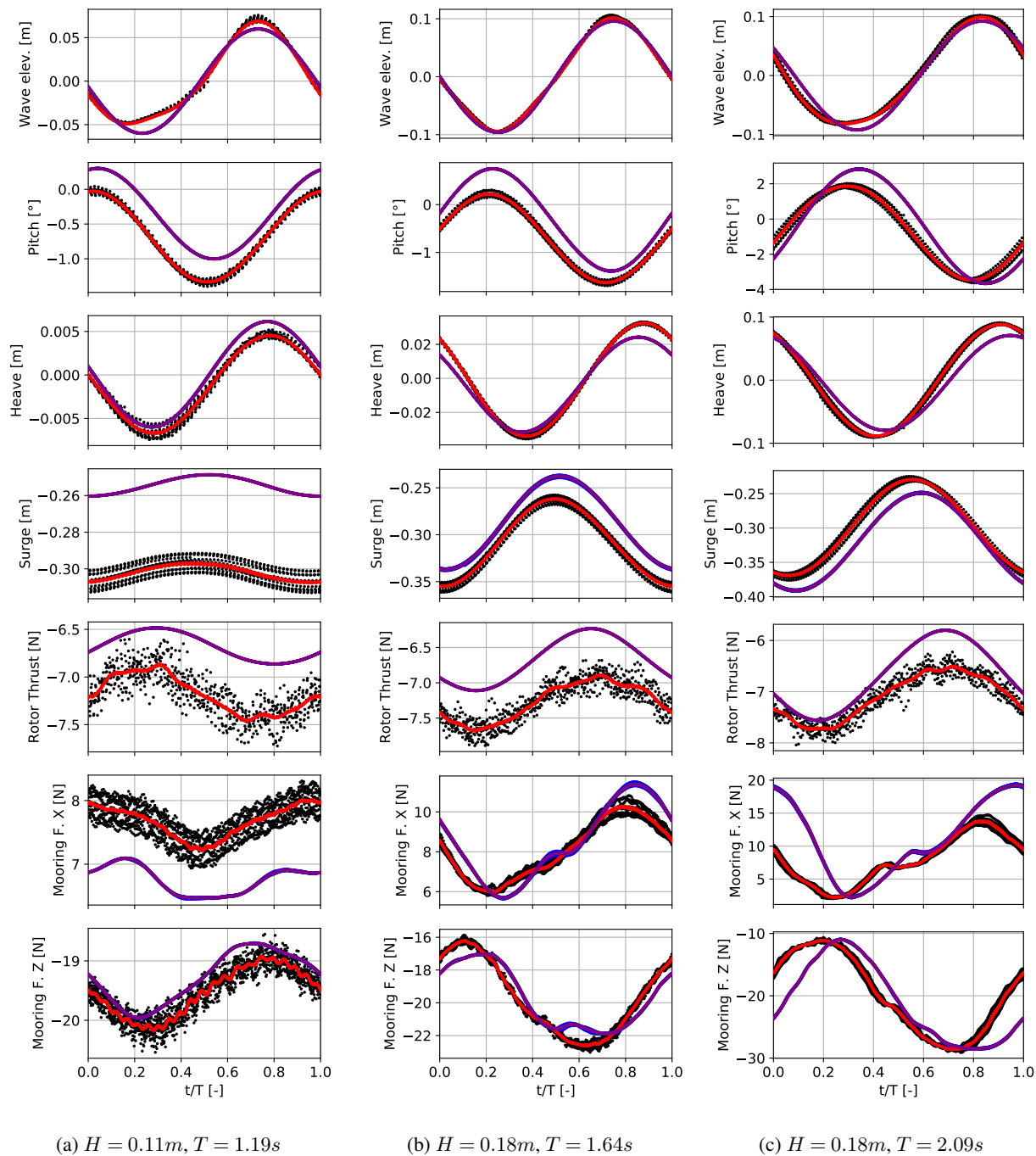
Figure 11. Waves and wind: Full simulations and experimental results at three different wave conditions. Experiment: ········· and ────── (averaged); Simulation: ········· and ────── (averaged).
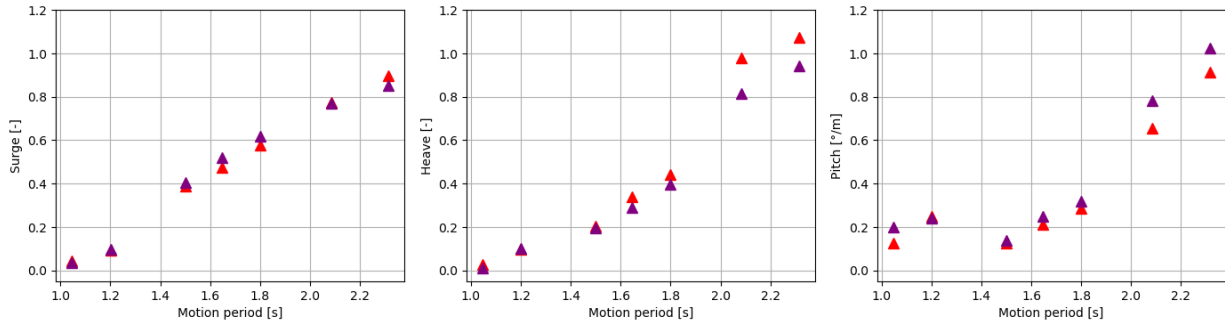
Figure 12. Waves and wind: Normalised motion amplitudes of regular wave and wind cases. Experiment: ▲, Simulation: ▲

agreement between measurements and simulations with slightly higher deviations at long wave periods can be concluded from the comparison of the normalised amplitudes.

8 Conclusions

In this study, the application of an improved testing and validation strategy for FOWT experiments and simulations is presented. Model tests of the CRUSE Offshore SelfAligner concept were performed in a wave basin, and the first-order panel method *pan*MARE is validated on the basis of the measurement data. In order to allow for a compensation of inertia and gravitational forces from the tower top loads revealing the aerodynamic rotor thrust force, a significant increase of the flow quality in comparison to conventional mobile wind generators was needed. This was achieved by an elaborate wind generator design, which would have been too large to fit the wave basin. Therefore, a reduction of the size of the wind turbine and thus the wind generator by a factor of three in comparison to common Froude scaling was applied. The consequences of the violation of scaling rules are discussed and found to be acceptable in exchange for a higher flow quality when aiming at the validation of a numerical method. A detailed description of the wind generator, the flow quality measurements, the model and the data acquisition system is given, and novelties are highlighted. The repetition error of motions, as well as aerodynamic thrust and mooring loads, is discussed in three exemplary cases. The validation is based on regular wave tests, which allow for the simple use of phase averaging in order to compare the measured quantities against simulations in time domain. Aside from the fully coupled simulations, hybrid simulations were performed to improve the distinction between causes and effects regarding differences between measurements and simulations, which is a general challenge in FOWT validations.

The findings from the validation of *pan*MARE can be summarised as follows:

– A mismatch of the mooring loads was the major driver of deviations between measurements and simulations. This was caused by an insufficient scaling of the catenary single point mooring due to the limited width of the towing tank. As a consequence, a highly dynamic behaviour of the mooring loads, which would not be expected in reality, was introduced and caused deviations in the mooring loads and, thus, the platform motion.

- A strong coupling of motions in heave, pitch and surge direction was introduced by the single point mooring. This coupling is characteristic for single point mooring structures. However, the insufficient scaling of the mooring system led to an over-representation of this effect.

- The simulated and measured aerodynamic loads showed very good agreement in time domain, which is a novelty for
525   comparisons of simulations with wave tank experiments of FOWT.

- Despite the scaling issue of the mooring system, an overall good agreement between measurements and fully coupled simulations could be achieved.

- The mean wave drift forces could not be modelled accurately by *pan*MARE. The inclusion of higher-order waves and a deformable free water surface in the model setup would most likely lead to significant improvements regarding surge
530   drift.

During the validation process, the following advantages and disadvantages of the proposed validation strategy were found:

- The repetition error of the platform motion could be reduced to a level slightly higher than the repetition error of the waves. Thus, only a marginal amount of random uncertainty was added to the measurements by the aerodynamic loading. This was achieved by the improved wind field and the reduction of the cable bundle to a single cable using wireless
535   data transfer. In addition, the systematic uncertainty could be reduced by the higher homogeneity and the precise characterisation of the wind field in comparison to other wind generators.

- The aerodynamic rotor thrust could be computed from the tower top force and compared to the simulations with a very low level of uncertainty. The low level of uncertainty in the platform motions and the wind field is a prerequisite for the applied compensation of the gravitational and inertial loads from the tower top loads.

540 - Performing hybrid simulations based on the measured platform motions together with the measurement of all relevant external loads turned out to be of major value because it allowed for the use of the exclusion principle. As a consequence, the sources of inaccuracies between measurements and simulations could be clearly identified in different load cases.

- Comparisons of all measured and simulated quantities using phase averaging allowed for the conservation of all relevant information from the measurements while random uncertainty was nearly completely eliminated. Additional value for
545   the validation arose from the possibility of identifying interrelations between the measured quantities during one motion cycle, which would be hampered when using statistical comparisons.

- The reduction of the rotor size, which was mandatory to achieve an improved flow quality, resulted in a significantly lower contribution of aerodynamic damping to the platform pitch motion. However, this contribution was well-defined and could be reproduced accurately in the simulations.

550   Finally, the proposed improvements to the validation process proved to be valuable in the presented case. The use of a smaller scaling ratio for the rotor than for the rest of the structure offers the chance to easily allow for an improved wind field quality.

In the present case, this offered further opportunities to improve the quality of the validation, such as the measurement of the rotor thrust force. Nevertheless, the reduced sensitivity of the rotor thrust to tower top motions violates the Froude similarity and needs to be evaluated carefully for the desired application case. In contrast to this, the measurement of interface loads 555 and hybrid simulations as well as comparisons of phase-averaged quantities most likely lead to an improved quality of the validation in any case provided that a sufficiently low level of random uncertainty can be reached. Although not done here, phase averaging can also be applied to irregular wave cases and together with an exact reproduction of the waves, the shown methodology can be extended to such cases easily.

Appendix A: Rotor scaling

560 Considering rotor thrust as the main aerodynamic load, the result of the scaling mismatch between the platform and the rotor can be approximated in a simplified way. In this case, the following simplifications need to be considered: The tower top motion velocity is low in comparison to the wind speed. The thrust coefficient is approximately constant for small changes in the effective wind speed seen by the rotor and independent of the derivative of the effective wind speed during a motion cycle. With these simplifications, the thrust force fluctuation amplitude due to a sinusoidal tower top motion in the surge direction 565 can be described as follows.

$$T_{amp,\lambda_{hydro}} = \frac{1}{4}\rho A_{\lambda_{hydro}} C_t \left(\left(u_{\lambda_{hydro}} + v_{tt,max} \right)^2 - \left(u_{\lambda_{hydro}} - v_{tt,max} \right)^2 \right) \tag{A1}$$

$$T_{amp,\lambda_{aero}} = \frac{1}{4}\rho A_{\lambda_{aero}} C_t \left(\left(u_{\lambda_{aero}} + v_{tt,max} \right)^2 - \left(u_{\lambda_{aero}} - v_{tt,max} \right)^2 \right) \tag{A2}$$

570 In equation A1 and A2, the thrust force fluctuation amplitude is approximated using Froude scaling ($T_{amp,\lambda_{hydro}}$) and the proposed further downscaling of the rotor ($T_{amp,\lambda_{aero}}$). $T_{amp,\lambda_{hydro}}$ is considered as a reference value reflecting the full-scale behaviour. ρ, A and C_t denote the air density, rotor swept area and nominal thrust coefficient. The wind speed according to Froude scaling is $u_{\lambda_{hydro}}$, while $u_{\lambda_{aero}}$ stands for the wind speed applied to the further downscaled rotor in the proposed setup. $v_{tt,max}$ denotes the maximum tower top surge velocity. As mentioned in section 3, it is mandatory to ensure that the absolute 575 value of the mean thrust $T_{\lambda_{hydro}}$ and $T_{\lambda_{aero}}$ remains the same during subscaling and at the same time TSR is kept constant. Therefore, the thrust coefficient remains unchanged. In other words, due to an increase in the inflow speed and the rotational speed, the absolute value of the thrust of the smaller rotor increases to the desired level while the operating point (TSR) is kept the same.

The ratio of the conventionally scaled and the further downscaled rotor thrust force fluctuation amplitude can be simplified 580 to:

$$\frac{T_{amp,\lambda_{aero}}}{T_{amp,\lambda_{hydro}}} = \frac{A_{\lambda_{aero}} u_{\lambda_{aero}}}{A_{\lambda_{hydro}} u_{\lambda_{hydro}}} \tag{A3}$$

As $A_{\lambda_{aero}}$ can be derived based on the increased scaling factor λ_{aero} and $u_{\lambda_{aero}}$ is determined by the ratio of the aerodynamic and hydrodynamic scaling factors, equation A3 can be simplified using the expressions in equation A4.

$$A_{\lambda_{aero}} = A_{\lambda_{hydro}}\left(\frac{\lambda_{hydro}}{\lambda_{aero}}\right)^2, u_{\lambda_{aero}} = u_{\lambda_{hydro}}\left(\frac{\lambda_{aero}}{\lambda_{hydro}}\right) \tag{A4}$$

585

$$\frac{T_{amp,\lambda_{aero}}}{T_{amp,\lambda_{hydro}}} = \frac{\lambda_{hydro}}{\lambda_{aero}} \tag{A5}$$

From equation A5, it is evident that the proposed approach leads to a reduced thrust force amplitude by a factor of $\lambda_{hydro}/\lambda_{aero}$.

590

Appendix B: Determination of mass and inertia properties

A considerable effort was invested to determine the weight and exact position of every part of the model, which includes all screws and cables. All measured weights and positions were fed into the CAD model in order to minimise the differences between the 3D model and the real model. Finally, the mass moments of inertia and exact COG position have been extracted

595 from the CAD model and applied to the simulation model. In order to give a hint on the reliability of this methodology, the model was placed on three pins with predefined positions, which were marked during the CNC manufacturing. Then, three scales were placed below the pins so that the COG position in the lateral plane could be computed from the weight measurements and the predefined distances. The difference between the lateral COG positions obtained in this way and from the CAD model turned out to be 1.4 mm and 2.2 mm respectively. Normalised to the platform length and width, this corresponds to

600 a relative deviation of 0.07 % and 0.18 %. Therefore, a low systematic uncertainty arising from differences in the mass moment of inertia and COG position is expected.

Appendix C: Sensing and data acquisition systems

C1 Sensing systems

A Vicon optical motion tracing system was utilised to capture the platform motion. The motion of a specialised marker geom-
605 etry consisting of reflecting spheres is computed from the pictures of three cameras positioned outside the towing tank by the processing unit. The horizontal alignment of the measured platform inclination was calibrated with a setup where the platform was aligned with the water surface. This was achieved by ballasting the platform so that all columns had the same draft, which was verified by an ultra-sonic-based distance sensor mounted above the floater model. The mooring forces have been measured using the three-component force sensor Althen ALF233, which fulfils the IP67 standard. A mould was milled on the lower
610 surface of the bottom plate during manufacturing to accommodate the sensor so that the shape of the underwater geometry

would not be altered when the sensor was mounted. Proper alignment in the yaw direction was reached with the aid of pin holes in the sensor and bottom plate. A me-systeme K6D six-component force/moment sensor was mounted directly below the nacelle in order to capture all relevant aerodynamic, inertial and gravitational loads. An ultra-sonic-based surface elevation sensor was placed at a defined position relative to the platform equilibrium position, but it was near the side of the tank in order to reduce the influence of wave reflections from the model in the measurements. The information on the exact sensor placement allowed for a precise application of the waves in the later simulations without the need for a phase shift correction. Hall sensors integrated into the Kollmorgen motor were utilised to measure the rotor speed of the wind turbine.

C2   Data acquisition systems

Two bluetooh-based wireless measurement amplifiers, me-systeme GSV6BT and GSV3BT, were utilised to transmit the tower top loads and mooing forces to the data acquisition computers. While the GSV3BT was placed inside the front column, the GSV6BT could be integrated into the tower top due to its low overall weight of approximately 100 g. The wave elevation sensor was operated with a land-based measurement amplifier. All measurement amplifiers, as well as the motion tracking system, were synchronised using a rectangular pulse triggered by a Wireless LAN signal. The only cable connection to the model had a diameter of approximately 7 mm and was necessary to control the motor of the wind turbine (see Figure 2). Therefore, a negligible contribution of the cable connection to the motion of the model is expected.

Author contributions.   CWS planned and conducted the experiment, developed the rotor thrust calculation procedure, conducted the validation and prepared the manuscript. SN conducted the simulations, made major contributions to the measurement data processing and reviewed the manuscript. PDK designed, manufactured and characterised the wind generator under the supervision of CWS and SN. MAM supervised all works and reviewed the manuscript.

Competing interests.   The authors declare no competing interests.

Acknowledgements.   The authors kindly thank the German Federal Ministry for Economic Affairs and Climate Action (BMWK) for funding the HyStOH project (03SX409A-F) and our partners CRUSE Offshore GmbH, aerodyn engineering GmbH, JÖRSS-BLUNCK-ORDEMANN GmbH, DNV- GL and the Institute for Ship Structural Design and Analysis at the Hamburg University of Technology for the excellent co-operation.

Furthermore, the authors thank CRUSE Offshore GmbH for supporting the manufacture and design of the FOWT model.

References

Ahn, H.-J. and Shin, H.: Model test and numerical simulation of OC3 spar type floating offshore wind turbine, International Journal of Naval Architecture and Ocean Engineering, 11, 1–10, https://doi.org/10.1016/j.ijnaoe.2017.09.010, 2019.

Amaral, G., Mello, P., do Carmo, L., Alberto, I., Malta, E., Simos, A., Franzini, G., Suzuki, H., and Gonçalves, R.: Seakeeping Tests of a FOWT in Wind and Waves: An Analysis of Dynamic Coupling Effects and Their Impact on the Predictions of Pitch Motion Response, Journal of Marine Science and Engineering, 9, 179, https://doi.org/10.3390/jmse9020179, 2021.

Andersen, M. T.: Floating Foundations for Offshore Wind Turbines, Ph.D. thesis, Aalborg University, https://doi.org/10.5278/VBN.PHD.ENGSCI.00175, 2016.

Azcona, J., Bouchotrouch, F., González, M., Garciandía, J., Munduate, X., Kelberlau, F., and Nygaard, T. A.: Aerodynamic Thrust Modelling in Wave Tank Tests of Offshore Floating Wind Turbines Using a Ducted Fan, Journal of Physics: Conference Series, 524, 012 089, https://doi.org/10.1088/1742-6596/524/1/012089, 2014.

Bergua, R., Wiley, W., Robertson, A., Jonkman, J., Brun, C., Pineau, J.-P., Qian, Q., Maoshi, W., Beardsell, A., Cutler, J., Pierella, F., Hansen, C. A., Shi, W., Fu, J., Hu, L., Vlachogiannis, P., Peyrard, C., Wright, C. S., Friel, D., Hanssen-Bauer, O. W., dos Santos, C. R., Frickel, E., Islam, H., Koop, A., Hu, Z., Yang, J., Quideau, T., Harnois, V., Shaler, K., Netzband, S., Alarcon, D., Trubat, P., Connolly, A., Leen, S. B., and Conway, O.: OC6 Project Phase IV: Validation of Numerical Models for Novel Floating Offshore Wind Support Structures, Wind Energy Science Discussions, pp. 1–36, https://doi.org/10.5194/wes-2023-103, 2023.

Bredmose, H., Lemmer, F., Borg, M., Pegalajar-Jurado, A., Mikkelsen, R., Larsen, T. S., Fjelstrup, T., Yu, W., Lomholt, A., Boehm, L., and Armendariz, J. A.: The Triple Spar campaign: Model tests of a 10MW floating wind turbine with waves, wind and pitch control, Energy Procedia, 137, 58–76, https://doi.org/10.1016/j.egypro.2017.10.334, 2017.

Cao, Q., Bachynski-Polić, E. E., Gao, Z., Xiao, L., Cheng, Z., and Liu, M.: Experimental and numerical analysis of wind field effects on the dynamic responses of the 10 MW SPIC floating wind turbine concept, Ocean Engineering, 261, 112 151, https://doi.org/10.1016/j.oceaneng.2022.112151, 2022.

Chen, P., Chen, J., and Hu, Z.: Review of Experimental-Numerical Methodologies and Challenges for Floating Offshore Wind Turbines, Journal of Marine Science and Application, 19, 339–361, https://doi.org/10.1007/s11804-020-00165-z, 2020.

Desmond, C., Hinrichs, J.-C., and Murphy, J.: Uncertainty in the Physical Testing of Floating Wind Energy Platforms' Accuracy versus Precision, Energies, 12, 435, https://doi.org/10.3390/en12030435, 2019.

Goupee, A. J., Fowler, M. J., Kimball, R. W., Helder, J., and de Ridder, E.-J.: Additional Wind/Wave Basin Testing of the DeepCwind Semi-Submersible With a Performance-Matched Wind Turbine, in: Volume 9B: Ocean Renewable Energy, p. V09BT09A026, American Society of Mechanical Engineers, San Francisco, California, USA, https://doi.org/10.1115/OMAE2014-24172, 2014.

Gueydon, S., Bayati, I., and de Ridder, E.: Discussion of solutions for basin model tests of FOWTs in combined waves and wind, Ocean Engineering, 209, 107 288, https://doi.org/10.1016/j.oceaneng.2020.107288, 2020.

Hall, M. and Goupee, A. J.: Validation of a hybrid modeling approach to floating wind turbine basin testing, Wind Energy, 21, 391–408, https://doi.org/10.1002/we.2168, 2018.

Hughes, S. A.: Physical Models and Laboratory Techniques in Coastal Engineering, vol. 7 of *Advanced Series on Ocean Engineering*, WORLD SCIENTIFIC, https://doi.org/10.1142/2154, 1993.

Jonkman, J.: Influence of Control on the Pitch Damping of a Floating Wind Turbine, in: 46th AIAA Aerospace Sciences Meeting and Exhibit, American Institute of Aeronautics and Astronautics, Reno, Nevada, https://doi.org/10.2514/6.2008-1306, 2008.

675 Murphy, J., Wright, C., Desmond, C., and Lynch, K.: Report on Physical Modelling Methods for Floating Wind Turbines, Tech. Rep. MARINET-D2.20, University College Cork, 2015.

Netzband, S., Schulz, C. W., Göttsche, U., Ferreira González, D., and Abdel-Maksoud, M.: A panel method for floating offshore wind turbine simulations with fully integrated aero- and hydrodynamic modelling in time domain, Ship Technology Research, 65, 123–136, https://doi.org/10.1080/09377255.2018.1475710, 2018.

680 Netzband, S., Schulz, C. W., and Abdel-Maksoud, M.: Self-aligning behaviour of a passively yawing floating offshore wind turbine, Ship Technology Research, 67, 15–25, https://doi.org/10.1080/09377255.2018.1555986, 2020.

Otter, A., Murphy, J., and Desmond, C. J.: Emulating aerodynamic forces and moments for hybrid testing of floating wind turbine models, Journal of Physics: Conference Series, 1618, 032 022, https://doi.org/10.1088/1742-6596/1618/3/032022, 2020.

Otter, A., Murphy, J., Pakrashi, V., Robertson, A., and Desmond, C.: A review of modelling techniques for floating offshore wind turbines, 685 Wind Energy, 25, 831–857, https://doi.org/10.1002/we.2701, 2021.

Robertson, A. N.: Uncertainty Analysis of OC5-DeepCwind Floating Semisubmersible Offshore Wind Test Campaign, in: Proceedings of the Twenty-seventh (2017) International Ocean and Polar Engineering Conference, 2017.

Robertson, A. N., Jonkman, J. M., Goupee, A. J., Coulling, A. J., Prowell, I., Browning, J., Masciola, M. D., and Molta, P.: Summary of Conclusions and Recommendations Drawn From the DeepCwind Scaled Floating Offshore Wind System Test Campaign, in: Volume 8: Ocean 690 Renewable Energy, p. V008T09A053, American Society of Mechanical Engineers, Nantes, France, https://doi.org/10.1115/OMAE2013-10817, 2013.

Robertson, A. N., Wendt, F., Jonkman, J. M., Popko, W., Dagher, H., Gueydon, S., Qvist, J., Vittori, F., Azcona, J., Uzunoglu, E., Soares, C. G., Harries, R., Yde, A., Galinos, C., Hermans, K., de Vaal, J. B., Bozonnet, P., Bouy, L., Bayati, I., Bergua, R., Galvan, J., Mendikoa, I., Sanchez, C. B., Shin, H., Oh, S., Molins, C., and Debruyne, Y.: OC5 Project Phase II: Validation of Global Loads of the DeepCwind 695 Floating Semisubmersible Wind Turbine, Energy Procedia, 137, 38–57, https://doi.org/https://doi.org/10.1016/j.egypro.2017.10.333, 14th Deep Sea Offshore Wind R&D Conference, EERA DeepWind, 2017.

Roddier, D., Cermelli, C., Aubault, A., and Weinstein, A.: WindFloat: A floating foundation for offshore wind turbines, Journal of Renewable and Sustainable Energy, 2, 033 104, https://doi.org/10.1063/1.3435339, 2010.

Schulz, C. W., Wang, K., Wieczorek, K., Netzband, S., and Abdel-Maksoud, M.: Experimental and numerical investigation of the yaw 700 moment of a downwind coned wind turbine rotor, Wind Energy, 25, 1995–2015, https://doi.org/10.1002/we.2779, 2022.

Schulz, C. W., Netzband, S., Özinan, U., Cheng, P. W., and Abdel-Maksoud, M.: Wind turbine rotors in surge motion: new insights into unsteady aerodynamics of floating offshore wind turbines (FOWTs) from experiments and simulations, Wind Energy Science, 9, 665–695, https://doi.org/10.5194/wes-9-665-2024, 2024.

Vittori, F., Azcona, J., Eguinoa, I., Pires, O., Rodríguez, A., Morató, A., Garrido, C., and Desmond, C.: Model tests of a 10MW semi-705 submersible floating wind turbine under waves and wind using hybrid method to integrate the rotor thrust and moments, Wind Energy Science, 7, 2149–2161, https://doi.org/10.5194/wes-7-2149-2022, 2022.

Wang, L., Bergua, R., Robertson, A., Wright, A., Zalkind, D., Fowler, M., Lenfest, E., Viselli, A., Goupee, A., and Kimball, R.: Experimental investigation of advanced turbine control strategies and load-mitigation measures with a model-scale floating offshore wind turbine system, Applied Energy, 355, 122 343, https://doi.org/10.1016/j.apenergy.2023.122343, 2024.

710 Wendt, F., Robertson, A., and Jonkman, J.: FAST Model Calibration and Validation of the OC5-DeepCwind Floating Offshore Wind System Against Wave Tank Test Data, International Journal of Offshore and Polar Engineering, 29, 15–23, https://doi.org/10.17736/ijope.2019.jc729, 2019.

Yu, W., Lemmer, F., Bredmose, H., Borg, M., Pegalajar-Jurado, A., Mikkelsen, R., Larsen, T. S., Fjelstrup, T., Lomholt, A., Boehm, L., Schlipf, D., Armendariz, J. A., and Cheng, P.: The Triple Spar Campaign: Implementation and Test of a Blade Pitch Controller on a
715   Scaled Floating Wind Turbine Model, Energy Procedia, 137, 323–338, https://doi.org/10.1016/j.egypro.2017.10.357, 2017.